Estimation of ^{235}U Mass in Natural and Depleted Uranium Samples With Different Matrix Materials Using the Active-Well Neutron Coincidence Counter

M. H. Hazzaa [1], W. I. Zidan [1], N. M. Ibrahiem [1], M. Y. Hassaan [2] and A. G. Mostafa [2]*

[1.] Egyptian Nuclear and Radiological Regulatory Authority (ENRRA), Department of Nuclear Safeguards and Physical Protection, Nasr City, P.O. Code 11762, Cairo, Egypt
[2.] ME Lab., Phys. Dept., Faculty of Science, Al-Azhar Univ., Nasr City, Cairo, Egypt
*drahmedgamal@yahoo.com

Abstract: An active-well neutron coincidence counter (AWCC) was applied to estimate ^{235}U mass by measuring the real coincidence count rate. Samples of different configurations and various chemical compositions were measured. This estimation was carried out via two main steps. Firstly, different experimental setup configurations (for the detector and samples) were modeled by Monte Carlo N-Particle transport code (MCNP-5) to calculate, numerically, the fission rates from nuclear material samples for each configuration. Secondly, the absolute efficiency of the detector was calculated using a standard sample of 1.068 kg natural uranium metal (of a cylindrical shape) to measure the neutron coincidence efficiency of the AWCC. Also other samples of 285.4 and 181.5 g of UF_4 and $(NH_4)_2U_2O_7$ respectively of natural uranium were also investigated. A semi-empirical calibration curve relates ^{235}U mass content in each modeled setup configuration with its corresponding measured real coincidence count rate was constructed. ^{235}U masses estimated from the calibration curve were found in agreement with the measured values within the limits of error. An accuracy better than 4.9% was achieved with an average precision of about 4%.
[Hazzaa MH, Zidan WI, Ibrahiem NM, Hassaan MY and Mostafa AG. **Estimation of ^{235}U Mass in Natural and Depleted Uranium Samples With Different Matrix Materials Using the Active-Well Neutron Coincidence Counter**. *Nat Sci* 2015;13(5):130-138]. (ISSN: 1545-0740). http://www.sciencepub.net/nature. 18

Keywords: Nucelar safeguards; Uranium mass content; Monte Carlo; Calibration of detector; AWCC

1. Introduction

According to the comprehensive safeguards agreement between a state and the internationl atomic energy agency (IAEA), it is the responsibility of the state to establish and maintain a state system of accounting for and control (SSAC) of all nuclear materials (NMs) anywhere under its authority [1]. The national objective of such a system is to account for and control all NMs in such state, and to contribute and detect any losses, unauthorized use or removal of any NMs [1, 2]. Consequently, the SSAC must have the capability to verify all NM types and categories in the state.

The basic measure of the SSAC is the NM accountancy [3] to verify quantitatively the amounts of NM presented. Non-destructive assay (NDA) techniques (employing neutron or gamma ray spectrometry) are widely used in such fields, especially for final product items and sealed or non-accessible containers and locations. Research and development activities aimed usually to improve NDA methods of interest for both the state and operators.

Uranium is one of the most important NMs, and hence its analysis is of great importance. Such analysis aims to determine the amount of uranium element in a sample and the mass ratio of the uranium isotopes. Passive NDA techniques, based on the analysis of the natural radioactive decay of gamma ray from the major isotopes of uranium, have been used in nuclear safeguards long time ago [4]. Due to the relatively low gamma ray energies and/or the low specific activities of the gamma-ray emitted from uranium isotopes (owing to its high density that increases its attenuation coefficient) the acquisition of the gamma spectrum is a lengthy procedure. This problem requires the estimation of some correction factors that may added a notable contribution to the uncertainty of the experimental results [5]. For such cases, NM assayed by neutron detection may be the preferred technique.

Fission neutrons are emitted in groups of two or more for each fission event. This signature could be detected as a neutron coincidence. Such coincidence counting system discriminates the background neutrons which are not correlated in time. Regarding the fissile isotope ^{235}U, the neutron generated from its spontaneous fission (2.99×10^{-4} n/s.g) is too low to be passively detected. Hence, an active system incorporating an external neutron source could be used to interrogate ^{235}U content by neutron induced fission [6].

The AWCC is a coincidence neutrons counting system. It was designed as non-destructively assay ^{235}U-bearing materials. If an Al- Cd sleeve is placed, the AWCC is said to be configured in the fast mode. The neutron spectrum is relatively of high energy, and the counter is suitable for assaying large

quantities of ^{235}U. While, if the Al-Cd sleeve is removed, the AWCC is said to work in the thermal mode [7].

The AWCC was tested and used in different applications by many authors, and they demonstrated its applicability for assaying uranium content in a wide variety of materials and generated calibration curves for different NM categories. Stationary and scanning measurements were performed with an AWCC to establish calibrations and performance specifications for the assay of ^{235}U and ^{235}U/cm for enriched uranium fuel assemblies [8]. El-Gammal et al proposed a semi-empirical method for ^{235}U mass calibration by using the AWCC [9]. Francesca Ferrari and Paolo Peerani have used neutron coincidence counting, NDA technique in nuclear safeguards to measure the mass of nuclear material in some samples. For high-enriched uranium (HEU) samples, active neutron interrogation is generally performed and the most common device used by nuclear inspectors is the AWCC [10]. Mykhaylov et al had obtained AWCC calibration curves for uranium metal and uranium dioxide with different enrichments up to 90 % [11].

In most of the published work, it was noticed that, to obtain accurate quantitative measurements, it is necessary to calibrate the instrument using physical standards representing the samples to be assayed. During field measurements it is expensive and difficult to obtain the large number of physical standards necessary to assay accurately the wide range of NM present at different locations. Generally, three different approaches might be used to address such issue; including semi-empirical calibration, cross calibration as well as Monte Carlo calculations.

However, in view of the lack of standard NMs, the estimation of ^{235}U mass content using the AWCC was proposed in this work using semi-empirical calibration. Some samples of natural uranium in the form of cylinders, and some others of depleted uranium (DU) cut from cylindrical segment which had been previously used as shielding material in a radiotherapy machine were used to estimate ^{235}U mass content.

The facility at which this work was carried out is the Nuclear Chemical Building –Egyption Atomic Energy Athuority, using their own NMs, where both are subject to the Safeguards Agreement between Egypt and the IAEA [MBA(ET-G), KMP(A)].

2. Methodology

The operation of the AWCC is based on the detection of timely correlated spontaneous or induced fission neutrons. For a uranium-bearing sample assayed in conventional coincidence counting with an AWCC, the relation between the total measured real coincidence count rate (R, s^{-1}) and the mass content of uranium isotopes of the assayed sample may generally take the form [9]:

$$R = \sum_x R_x = \sum_x M_x \cdot F_x^m \cdot f_{cx} \quad (1)$$

where R_x is the real coincidence count rate due to isotope x (s^{-1}), M_x is the mass of isotope x (g), F_x^m is the total specific fission rate of the isotope x (fissions/s g) and f_{cx} is the counter coincidence counting efficiency of the isotope x [9].

Only the thermalized AmLi neutrons will interrogate the ^{235}U nuclei. Hence, equation (1) will be reduced to,

$$R = M_5 \cdot F_5^m \cdot f_{c5} \quad (2)$$

where M_5 is the ^{235}U mass of the sample (g),F_5^m is the ^{235}U specific induced fission rate (fissions/s g) and f_{c5} is the counter coincidence counting efficiency of ^{235}U fission neutrons.

For a sample of cylindrical shape, with a relatively small radius "r", its volume could be divided into small elements in the form of discs with radii equal to that of the sample and heights "dz". Due to the small diameter of the sample, the change in fission rate and efficiency along the sample diameter could be ignored. In this case, if the sample axis of symmetry is parallel to the z-axis, therefore equation (2) becomes

$$R = \pi\, r^2 M_5 \int_a^b F_5^{\nu}(z) \cdot f_{c5}(z)\, dz \quad (3)$$

But if the sample takes the rectangular shap, the sample is divided into infinitesimal elements of nearly equal volumes (dv's), where (dv=A.dz), then equation (2) becomes,

$$R = A\, M_5 \int_a^b F_5^{\nu}(z) \cdot f_{c5}(z)\, dz \quad (4)$$

where (A) is the area of the base for an element of volume. Where the limits of integration a and b represent the locations of the first and last element of the volumes along the effective length of the sample.

It was mentioned before that, in case of the absence of standard NMs, $F_5^{\nu}(z)$ and $f_{c5}(z)$ in Eqns. (3, 4) have to be measured or calculated. Monte Carlo calculations could be applied to predict $F_5^{\nu}(z)$function [12, 13].

In this study, a characterized stander uranium sample, has a cylindrical shape, of 1.068 kg natural uranium metal was used to measure the neutron coincidence efficiency of the AWCC. Also, two samples of natural uranium (285.4 and 181.5 g) of UF_4 and $(NH_4)U_2O_7$ respectively were also measured. The function $f_{c5}(z)$ in Eqns. (3, 4) could be replaced by that deduced with the stander samples.

Once the fission rate function is determined, the coincidence efficiency and the real coincidence count rate can be measured, and a calibration curve can be obtained giving the relation between the real coincidences count rate and ^{235}U mass content.

3. Experimental

3.1. System setup

An AWCC system [Canberra, Model JCC-51] consists of a high-density polyethylene ring in which 42 ^{3}He thermal-neutron detectors [Reuter-Stokes model RS-P40820-103] are mounted in two concentric circles. The detectors are wired to give six groups of seven tubes for each. Each group is ganged through a single preamplifier/amplifier/discriminator board [JAB-01 Amptek]. The board output pulses are analyzed by the neutron analysis shift register [model JSR-141] with the detector parameters shown in Table (1). The system consists of two $^{241}AmO_2$-Li neutron sources (7.6×10^4 n/s emission rate for each) to activate thermal fission in an assayed samples. Each source is kept in a stainless steel container. A tungsten shield is placed around each neutron source to reduce the gamma-ray emission [14-16].

Table 1. Detector parameters and timing characteristics used for this work [9]

Gate width	64 μsec
Predelay time	4.5 μsec
High voltage	1680 V
Die-away time	52.36 μsec

The AmLi neutron sources were positioned at 17.3 and 50.3 cm (upper and lowerlocations of the detector) from the bottom of the detector to allow optimum sample interrogation. Al-Cd sleeves are removed from the detector cavity in order that, the counter operates in the active thermal mode. The measuring setup parameters for data acquisition are adjusted using Canberra NDA2000 Software [17].

3.2. Measurement of coincidence efficiency using standard uranium sample

The coincidence efficiency of the AWCC in the active-thermal mode has been estimated via measuring the ^{235}U real coincidence count rate of the characterized stander uranium sample and calculating its induced fission rate by using MCNP-5 code.

3.2.1. Real coincidence count rate measurements

To measure the real coincidence count rate of the characterized standard uranium sample, it has been located inside the cavity of the counter according to the active-thermal mode configuration set up (Fig. 1). It has been measured for uranium metal at eight different locations for 28800 sec for each. For $(NH_4)_2U_2O_7$ and UF_4 matrices the measurements were carried out at seven different locations and three runs were taken for each location.

3.2.2. Induced fission rate calculations

The induced coincidence fission rate of the characterized standard uranium sample has been estimated by MCNP code. The ^{235}U fission rate calculations were performed such that the sample locations inside the cavity of the counter cover those locations at which the measurement were done.

The coincidence efficiency of the detector was calculated as the ratio of the average real coincidence count rate to the fission rate of the characterized standard uranium sample. The obtained values of the coincidence efficiency at different locations were fitted against the experimental measurements in order to obtain the function $f_c(z)$ which represents the coincidence efficiency of the detector.

3.3. Nuclear material measurements

Three rectangular pure metallic DU samples of 17.15 cm height and 3.2 cm length and 1.65 cm width, three cylinders of 18.2 cm length and 6 cm diameter containing powder natural $(NH_4)_2U_2O_7$ and other three cylinders of the same dimensions containing powder natural UF_4, have been used to measure the real coincidence neutrons count rate of ^{235}U. Tables (2 3, and 4) present the physical characteristics of these samples. Fig. (2), illustrates the different setup configurations of the AWCC for which the NM samples were measured. For each setup configuration, the real fission coincidence neutrons is calculated as the average of three measurements. The uncertainties for the coincidence counting rates ranged between 1.2% and 5% according to the number of measured cylinders and rectangular samples (from one to three cylinders and rectangular). The measuring times were 2400 sec.

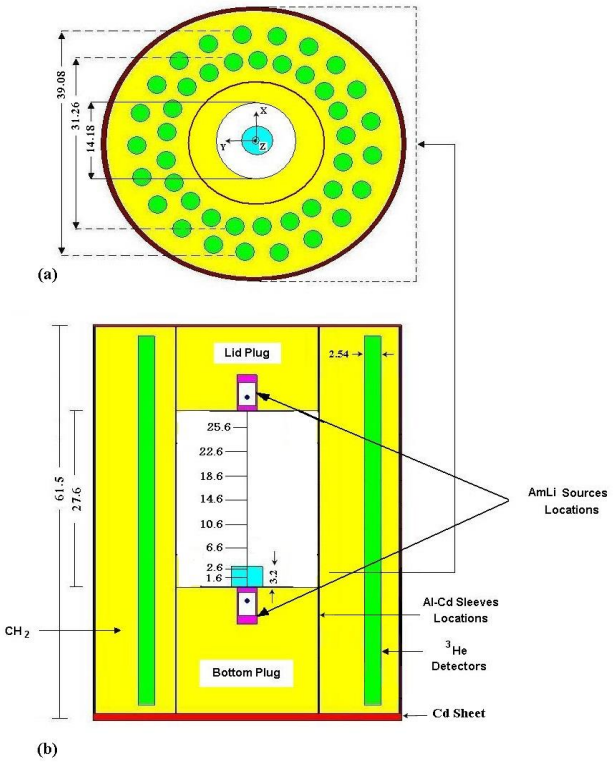

Figure 1. Experimental setup configuration for 1.068 kg NU metal sample measured inside the detector cavity to obtain the efficiency in active thermal mode by removing the insert Al-Cd sleeves (a) Cross sectional view, (b) longitudinal view.

Table 2. Physical characteristics of the NM samples for $(NH_4)_2U_2O_7$ matrix

Sample#	Net weight, g	Weight of ^{235}U, g
1	466.62	3.359
2	436.79	3.145
3	446.78	3.217

Table 3. Physical characteristics of the NM samples for (UF_4) matrix

Sample#	Net weight, g	Weight of ^{235}U, g
1	755.92	5.443
2	843.76	6.075
3	810.49	5.836

Table 4. Physical characteristics of the NM samples for DU metal

Sample#	Net weight, g	Weight of ^{235}U, g
1	1447.8	6.226
2	1445.3	6.215
3	1445.5	6.216

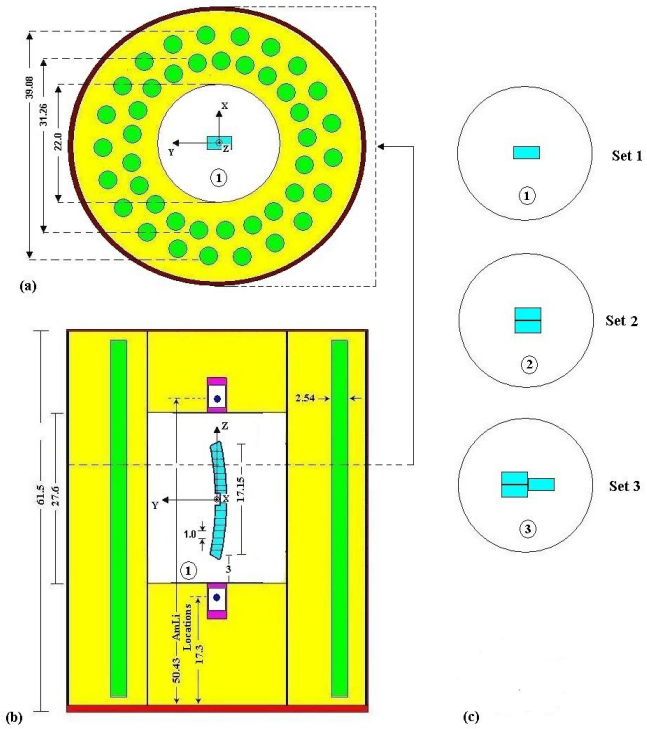

Figure 2. Geometrical model of the AWCC used for Monte Carlo calculations with different setup configurations of DU metal samples inside the cavity. (a) Cross sectional view, (b) longitudinal view and (c) different setup configuration for different sets.

4. Fission rate calculation

Fission rate ($F_5^{\nu}(z)$ function in Eqns. 3 & 4) of ^{235}U nuclei in NM samples measured by the AWCC depends on many parameters and factors including physical characteristics of all materials involved, configuration of the experimental setup and interaction cross sections of interrogation neutrons with different materials. Monte Carlo modeling is an efficient and accurate method to calculate the fission rate using the multi-purpose MCNP-5 code via NM-detector geometry modeling (as shown in Fig. 2) [18]. Locations, dimensions, effective lengths and ^{3}He properties and AmLi source activities were all obtained from references [7, 15, 16]. The density of the polyethylene moderator was determined from the measured mass and volume of the top plug. The AmLi neutron source was assumed to be a point source. Its mean energy used in the simulation process is 0.451 MeV [19].

Fission rate per unit volume was calculated using the track length estimation of the cell flux (F4:N n) with the tally multiplier card (FMn C M R_1), where n is the cell number (which contains the NM), C is the atomic density of the material, M is the material number on material card and R_1 is the

reaction number for total fission cross section, (R_1 = -6).

The fission rate depends on the location of the source, which is not uniform along the NM sample. However, to obtain the function which describes the fission rate along the sample length ($f_5^{v}(z)$), the rectangular samples were divided into seventeen small segments of equal heights (about 1.01 cm for each), while the cylindrical samples were devided to eighteen small segments of equal heights (about 1.01 cm for each also). Then the fission rate was calculated for each segment of both shapes. This process was repeated for each NM sample in each setup configuration. Each calculational run was performed using 10^6 histories; the time of the run was about 20 min on a 2.2 GHz Core 2Duo processor. The relative standard deviation of the MCNP calculations did not exceed 2.6% for all runs.

5. Results and Discussion

The estimation of ^{235}U mass obtained by a characterized standard uranium sample to assay the NM samples was performed by measuring the real coincidence count rate efficiency of the detector and the fission rate for NM samples.

Figs. (3, a-c), illustrate the variation of the coincidence efficiency ($f_c(h)$) of the detector as a function of the position inside the AWCC cavity. The values of the measured efficiency at the middle of the detector were found to be 0.714, 0.381 and 0.108 for $(NH_4)_2U_2O_7$, UF_4 and DU metal samples respectively. As the detector was moved towards each of the detector ends, these values exhibit sharp decrease to reach 0.323, 0.234 and 0.066 respictively. This sharp variation reflects the effect of the increase of the neutron leakage probability at the open ends and the coincidence efficiency variation with the power of multiplicity. The illustrated uncertainties is due to statistical error in the coincidence count rate. The experimental data were fitted to a three-order polynomial functions [Eqns. (5, 6 & 7) for $(NH_4)_2U_2O_7$, UF_4 and DU metal matrices respectively],

$$f_c(h) = 0.14532 + 0.10802\,h - 0.00587\,h^2 + 6.6907\times10^{-5}\,h^3 \quad (5)$$

$$f_c(h) = 0.16192 + 0.03838\,h - 0.00184\,h^2 + 1.26649\times10^{-5}\,h^3 \quad (6)$$

$$f_c(h) = 0.05352 + 0.00877\,h - 3.51965\times10^{-4}\,h^2 + 9.05397\times10^{-7}\,h^3 \quad (7)$$

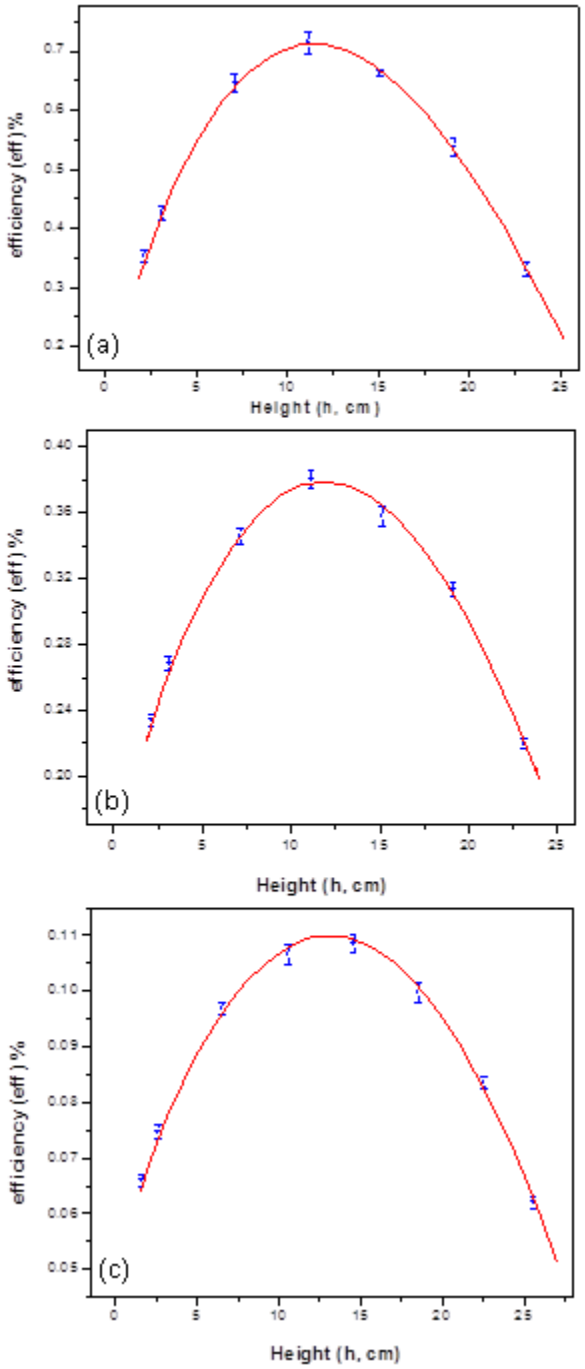

Figure 3. The variation of the measured coincidence efficiency of the detector using the characterized sample with location inside the detector cavity for (a) $(NH_4)_2U_2O_7$ matrix (b) UF_4 matrix (c) DU metal.

Assuming uniform radial coincidence efficiency, of the form

$$R = \pi\, r^2 S\; M_5 \int_a^b f_5^{v}(z)\cdot f_c(z)\, dz \quad (8)$$

Where (S) is the interrogation neutron source activity (neutron/s), Eqn. (8) could be used to estimate the ^{235}U mass due to thermal induced fissions for NM samples at any location, inside the cavity of the detector position, taking into consideration that the sample characteristics verify the condition that $f_{c5}(z)$ is equal to $f_c(z)$. Moreover, due to variation of the fission rate with the position inside the cavity of the detector, the function $f_5^v(z)$ must be recalculated at different locations. Consequently, different setup configurations (Fig. 2(b)), will be also considered.

For each setup configuration in Fig. 2(b), the value of $f_5^v(z)$ was calculated for all divisions of both the rectangular and cylinderical shapes using MCNP code. In Fig. 2 (a) the setup configuration number "1" is illustrated for fission rate calculations inside the NM sample number "1".

Figs. (4, a-c) show the variation of the calculated fission rate per unit volume per sample division with location, for each NM sample of the three different setup configurations (as exhibited in Fig. (2)), for $(NH_4)U_2O_7$, Figs. 5 (a-c) for UF_4 and Figs.6(a-c) for DU metal matrices.

It is clear from Figs. 4 (a-c), 5 (a-c) and 6 (a-c) that the fission rate depends not only on the location of the sample inside the cavity of the detector but also on the locations of the other samples as well. For each sample, fission rate calculations yield is a function characterized with three peaks. The variation of the fission rate with location was described by a function of superimposed three Gaussian functions. The fission rates have the maximum values at the ends of the cavity (upper and lower) where the interrogation AmLi neutron sources are located. It is clear from Figures 4 (a-c), 5 (a-c) and 6 (a-c) that the values of the calculated induced fission rate exhibit a notably decrease at the middle of the sample. This is due to the small volumes of the NM divisions at the middle of the samples as shown in Fig. 2 (b). The deduced fission rate function composed of three Gaussian functions is given by:

$$f_5^v(z) = F_{r_0} + \sum_{j=1}^{3}\left(\frac{A_j}{w_j \cdot \sqrt{\pi/2}}\right) \cdot Exp\left(\frac{-2(z - zc_j)^2}{w_j^2}\right) \quad (9)$$

where Fr_o, A_j, w_j and zc_j ($j=1,2,3$) are the parameters of the three Gaussian functions.

The fitting curves are illustrated in Figs. 4 (a-c), Figs. 5 (a-c), and Figs. 6 (a-c).

The ^{235}U mass content in $(NH_4)U_2O_7$ and UF_4 as well as in DU metal matrices can be calculated by substituting Eqns. (5, 6, 7 and 9) in Eqn. (8) and using the real count rates obtained from the experimental work which leads to calculate the ^{235}U mass for $(NH_4)U_2O_7$ and UF_4 from equation (10) and for DU metal from equation (11),

$$M_5 = \frac{R}{\pi r^2 S \sum_{i=1}^{n} \int_{3}^{21,2} f_{c5}(h).(Fr_0 + \sum_{j=1}^{3} \frac{A_{ij}}{w_{ij}\sqrt{\frac{\pi}{2}}} e^{-2\frac{(h-h_{cij})^2}{w_{ij}^2}}).dh} \quad (10)$$

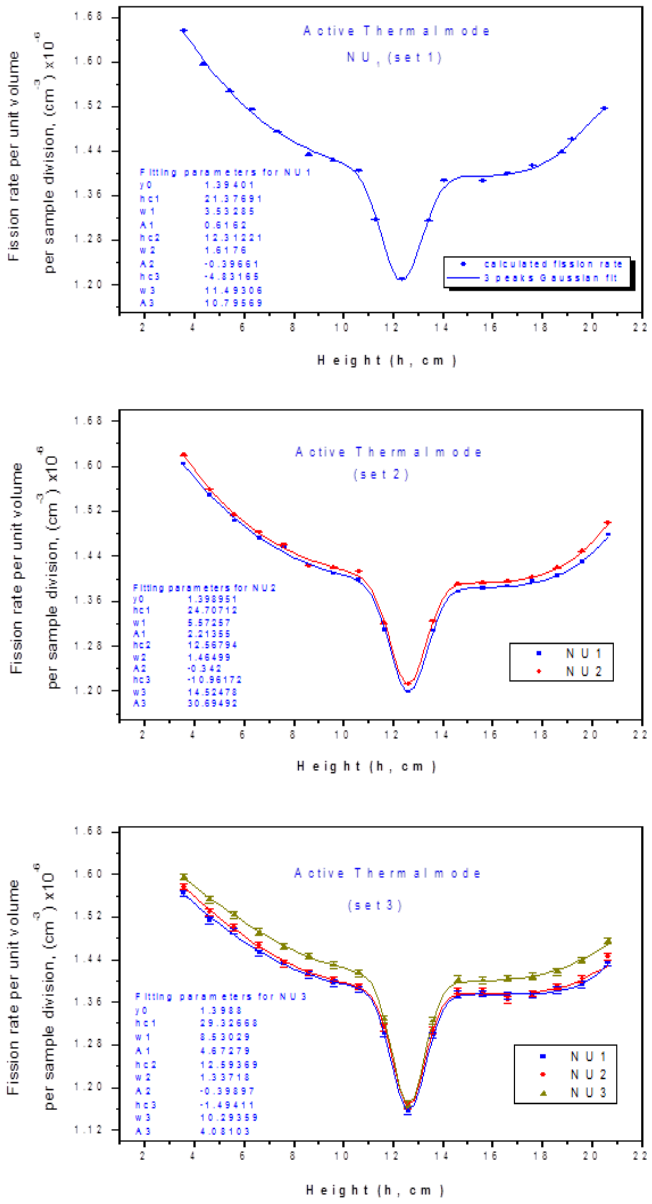

Figure 4 (a-c). The calculated fission rates per unit volume per NM sample division for each sample and setup configuration for (UF_4) matrix.

$$M_5 = \frac{R}{AS\sum_{i=1}^{n}\int_{3}^{20.15} f_{c5}(h).(Fr_0 + \sum_{j=1}^{3}\frac{A_{ij}}{w_{ij}\sqrt{\frac{\pi}{2}}}e^{-2\frac{(h-h_{cij})^2}{w_{ij}^2}}).dh} \quad (11)$$

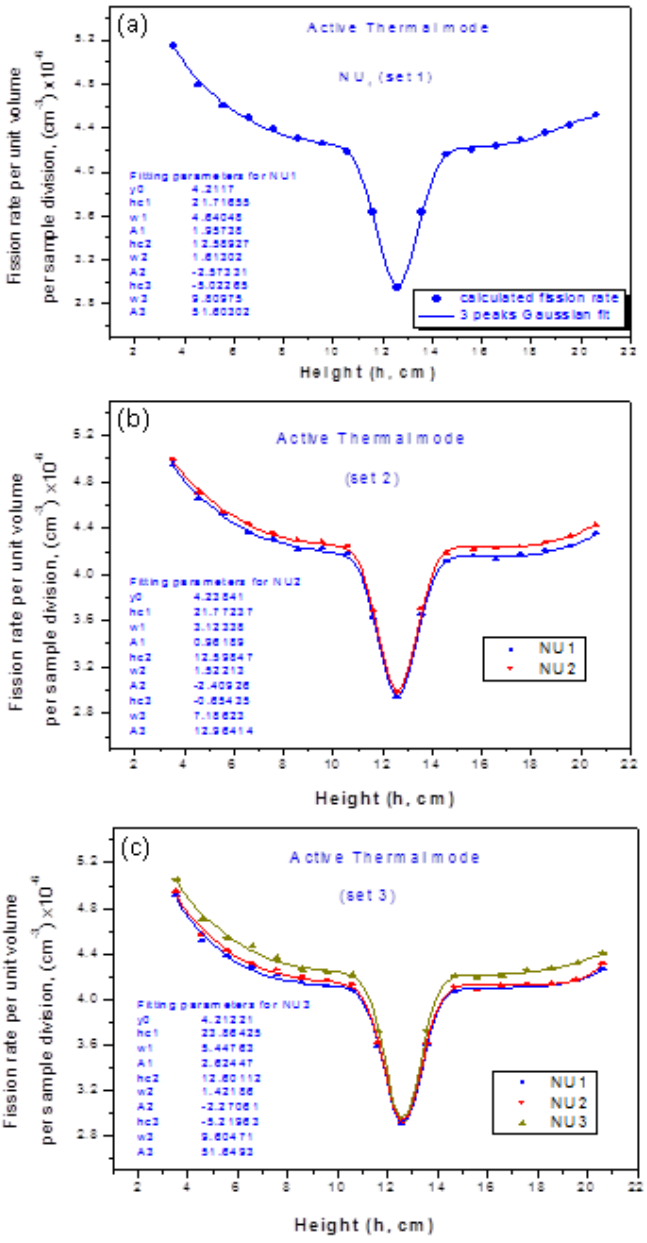

Figure 5 (a-c). The calculated fission rates per unit volume per NM sample division for each sample and setup configuration for UF_4 matrix.

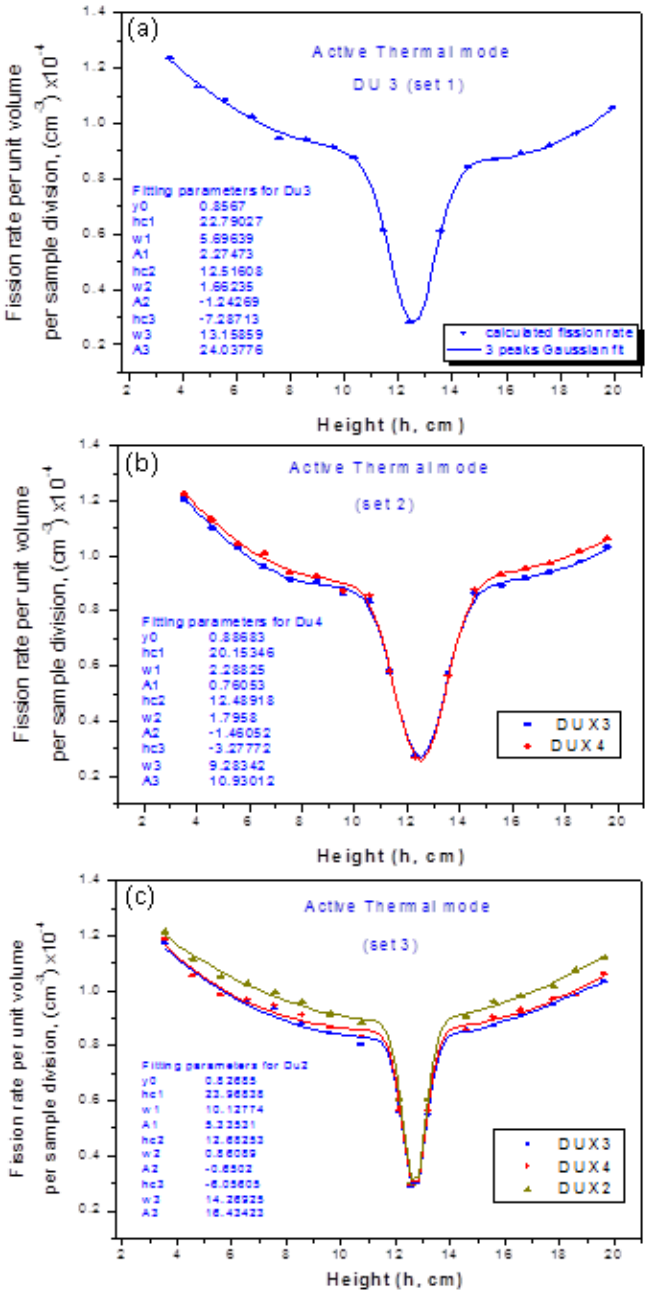

Figure 6 (a-c). The calculated fission rates per unit volume per NM sample division for each sample and setup configuration for DU metal.

Fig. (7), shows the results of the real coincidence count rate as a function of ^{235}U mass content corresponding to each setup configuration. A second order polynomial fitting was applied to construct the calibration curve, which can be obtained using Eqns. (12, 13 and 14) for $(NH_4)_2U_2O_7$, UF_4 and DU metal matrices respectively.

$$M_5 = 2.36639 + 0.03046\,R + 8.75632\times10^{-5}\,R^2 \quad (12)$$

$$M_5 = -0.20992 + 0.05147\,R - 2.75665\times10^{-6}\,R^2 \quad (13)$$

$$M_5 = 2.36639 + 0.03046\,R + 8.75632\times10^{-5}\,R^2 \quad (14)$$

These equations (12, 13 and 14) represent the calibration curves obtained by semi-empirical calibration of the AWCC.

^{235}U mass content was calculated via substituting the measured real coincidence count rates in Eqns. (10, 11) and Tables (5, 6 and 7) presents the measured and calculated ^{235}U mass content for different setup configurations with precision and relative accuracy. The estimated values were found to be in agreement with the measured ones within the limits of error.

The uncertainty of the estimated ^{235}U masses result from the calculated uncertainty in the calibration curve represents statistical errors due to MC calculations and the uncertainty in the measured coincidence efficiency. The uncertainty in the measured mass is composed of two components; a systematic error due to uncertainty in the ^{235}U enrichment value and a statistical random error in the weighing balance.

Table 5. Measured and calculated ^{235}U mass for the $(NH_4)_2U_2O_7$ matrix

Setup config. #	Measured mass (M) ± σ_M	Estimated mass (M_5) ± σ_{M5}	Relative accuracy %
1	3.359±0.084	3.462±0.105	-3.07
2	6.505±0.162	6.610±0.156	-1.61
3	9.721±0.463	9.379±0.352	3.52

Table 6. Measured and calculated ^{235}U mass for the UF_4 matrix

Setup config. #	Measured mass (M) ± σ_M	Estimated mass (M_5) ± σ_{M5}	Relative accuracy %
1	5.443±0.176	5.662±0.069	-4.02
2	11.518±0.289	11.396±0.123	1.06
3	17.353±0.435	16.682±0.364	3.86

Table 7. Measured and calculated ^{235}U mass for the DU metal

Setup config. #	Measured mass (M) ± σ_M	Estimated mass (M_5) ± σ_{M5}	Relative accuracy %
1	6.226±0.264	6.501±0.285	-4.42
2	12.440±0.362	12.841±0.503	-3.22
3	18.656±0.478	18.032±0.584	3.34

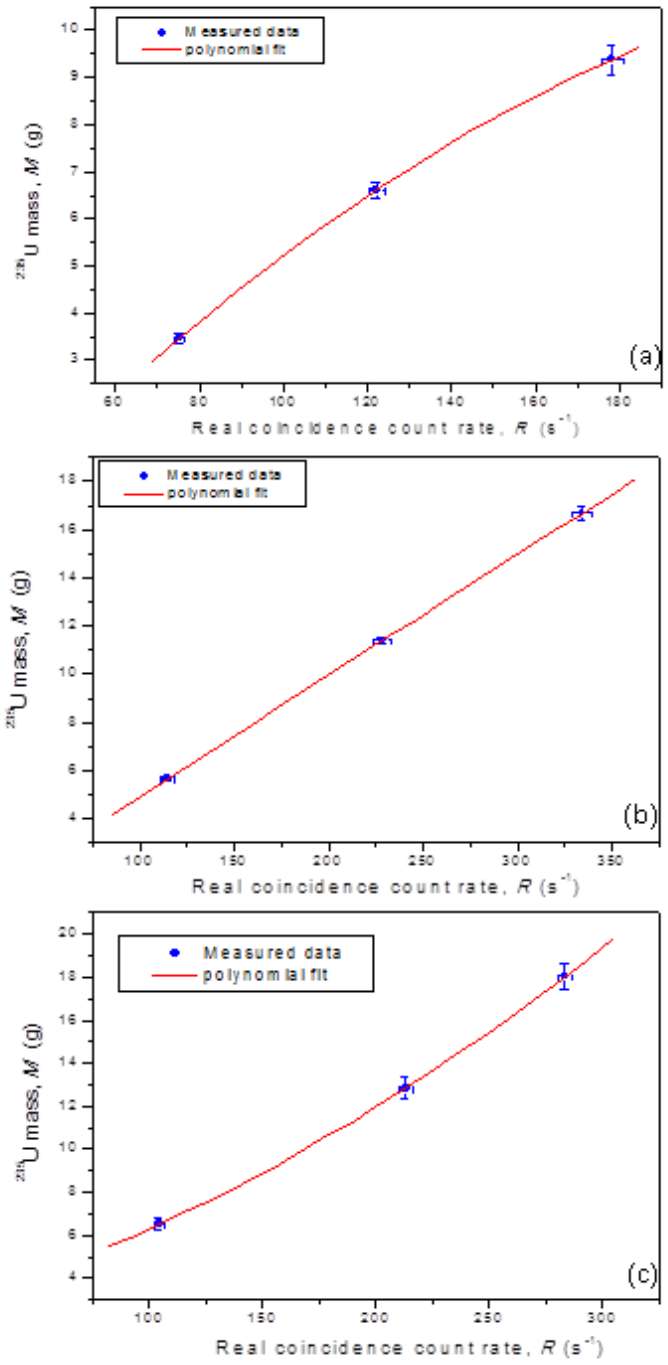

Figure 7. The variation of the real coincidence count rate with ^{235}U mass. Solid line represents the second order polynomial fit of the estimated data (a) $(NH_4)_2U_2O_7$ matrix, (b) UF_4 matrix and (c) DU metal.

5. Conclusion

The estimated ^{235}U mass contents in NM samples are found in agreement with the measured values within the limits of error. The accuracy and average precision of the present method were found to be better than 4.9% and 4%, respectively. This method depends on the combination of the experimental measurements of the coincidence efficiency of the detector with MCNP code calculations to estimate ^{235}U mass content in NM samples.

It is seen also that, more investigation is still needed to improve the accuracy and precision of the proposed method. This could be achieved through performing a series of more precise measurements of the detector efficiency. It is also expected that more reliable results could be achieved if complete information about interrogation sources are available.

Corresponding Author:
Prof. Dr. Ahmed G. Mostafa
ME Lab., Phys. Dept.
Faculty of Science
Al-Azhar Univ., Nasr City, Cairo, Egypt
E-mail: drahmedgamal@yahoo.com

References

[1] The structure and content of agreements between the agency and states required in connection with the nonproliferation treaty of nuclear weapons, IAEA Doc. INFCIRC/153 (Corr.), IAEA,Vienna, Austria (1972).

[2] Guidelines for states' systems of accounting for and control of nuclear materials, IAEA/SG/INF/2, IAEA, Vienna, Austria (1980).

[3] Safeguards techniques and equipments, International nuclear verification series No.1, IAEA,Vienna, Austria (1997).

[4] T. D. Reilly, N. Ensslin, H. A. Smith and Jr. S. Kreiner, "Passive nondestructive assay of nuclear materials", Los Alamos National Laboratory, USA Regulatory Commission, NUREG/CR-5550, LA-UR-90-732 (1991).

[5] W. El-Gammal, M. El-Nagdy, M. Rizk, S. Shawky and M. A. Samei, Nucl. Instr. and Meth. (A), 553 (2005) 627.

[6] N. Ensslin, W. C. Harker, M. S. Krick, D. G. Langner, M. M. Pickrell and J. E. Stewart, Application Guide to Neutron Multiplicity Counting, Los Alamos National Laboratory, (LA-13422-M) (1998).

[7] H. O. Menlove, Description and operation manual for the active well coincidence counter, Los Alamos National Laboratory, (LA-7823-M) (1979).

[8] M. S. Krick, L. Cowder, V. Maltsev, A. Chernikov, P. Mokeenko, K. D'yadkov, V. Ivanov, A. Lagattu, Y. Lopatin, K. Czock, D. Rundquist and L. Pedraza, the 13th ESARDA symposium on safeguards and nuclear material management, (LA-UR--91-1568), Avignon (France) 14-16 May (1991).

[9] W. El-Gammal, W. I. Zidan and E. Elhakim, Nucl. Instr. and Meth. (A), 565 (2006) 731.

[10] Francesca Ferrari and Paolo Peerani, Radiation Measurements, 45 (2010) 1034.

[11] V. Mykhaylov, M. Odeychuk, V. Tovkanetz, V. Lapshyn, K. Thompson and J. Leicman, Symposium on international safeguards, (IAEA-SM-367/4/04/p), Vienna, Austria, 29 Oct - 2 Nov, 33 (2001).

[12] K. Böhnel, "Determination of plutonium in nuclear fuels using the neutron coincidence method", KfK-2203, Karlsruhe (1975) [(English trans.: AWRE TRANS 70 (54/4252) Aldermaston (1978)].

[13] M. S. Krick and H. O. Menlove, The high-level neutron coincidence counter (HLNCC): Users' Manual, (LA-7779-M) (1979).

[14] CANBERRA, Active well neutron coincidence counter, Model JCC-51, User's manual, USA (1998).

[15] CANBERRA, Neutron coincidence counter checklist, ^{3}He tube data sheets, USA (1998).

[16] CANBERRA, Neutron analysis shift register, Model JSR-14, User's manual, USA (1997).

[17] CANBERRA, NDA 2000 Non-Destructive Assay Software, USA (2006).

[18] Jeremy E. Sweezy (MCNP Team Leader.), MCNPTM—A general Monte Carlo N-particle transport code (Version 5), (LA-12625-M), April 24 (2003) (Revised 10/3/05)

[19] H. Tagziria, N. J. Roberts and D. J. Thomas, Nucl. Instr. And Meth. A, 510 (2003) 346.

4/22/2015